epl draft

Conditional phase-shift enhancement through dynamical Rydberg blockade

Jin-Hui Wu[1], M. Artoni[2,3], F. Cataliotti[2,4] and G. C. La Rocca[5]

[1] Center for Quantum Sciences and School of Physics, Northeast Normal University, Changchun 130024, China
[2] European Laboratory for Nonlinear Spectroscopy (LENS), 50019 Firenze, Italy
[3] Department of Engineering and Information Technology and INO-CNR Sensor Lab, Brescia University, 25133 Brescia, Italy
[4] Department of Physics and Astronomy, University of Florence, 50019 Firenze, Italy
[5] Scuola Normale Superiore and CNISM, 56126 Pisa, Italy

PACS 42.50.Gy – Electromagnetically induced transparency
PACS 32.80.Ee – Rydberg states
PACS 42.65.-k – Nonlinear optics

Abstract – Large cross-phase shifts per photon can be attained through an all-optical polarization control of dipole blockade in Rydberg atoms. A pair of weak circularly-polarized signal and control light pulses experience a giant nonlinear cross-interaction through the conditional excitation of a Rydberg state. Conditional cross-phase modulations on the order of π-radians may be attained under specific symmetric EIT quasi-resonance conditions at large degrees of transparency. We also address the possibility of extending our scheme to work at very low intensities and within a few-blockade-radii regions.

Introduction. – Photons are ideal carriers of information because they can easily be transmitted over long distances and loosely couple to the environment, yet their use is often largely hampered by the absence of significant photon-photon interactions especially when *cross-phase* nonlinearities are needed [1, 2]. Effective interactions between photons must be then mediated by a suitable medium to reach useful cross-phase shifts. For potential applications in advanced optical information processing [3] one is required to deal with conditional nonlinear interactions that are enabled when a "control" light pulse imprints a phase shift onto another "signal" light pulse [4]. Promising strategies consist in coupling an optical cavity to single atoms [5, 6], atomic ensembles [7], and artificial atoms [8]. Alternative approaches comprise light-atoms interfaces [9] driven into a regime of electromagnetically induced transparency (EIT) [10]. These implementations, however, are challenging and the observed cross-nonlinearities yield conditional phase shifts far less than the desired value of π [11, 12]. Cross-phase modulations in the range $1 - 10$ micro-radians per photon have been observed in slow-light cold atoms [13] while slightly larger shifts have been achieved through specific post-selection procedures [14].

Rydberg atoms have attracted extensive attention owing to the presence of strong dipole-dipole interactions [15, 16]. These manifest themselves directly through a dipole blockade effect [15, 17] preventing the simultaneous excitations of two or more atoms within a Rydberg superatom (*SA*) [18]. Such a mechanism has been exploited to create robust light-atoms interfaces [9, 19, 20] where the combination with EIT makes Rydberg media appealing to foster significant cooperative optical nonlinearities [7, 16, 21, 22]. Recently a single-photon π phase-shift has been measured in such Rydberg-EIT media through a pulse storage-retrieval technique [23], as well as in high-finesse optical resonators for atoms [24,25]. Note, however, that the π phase-shift in [23] is postselected upon the detection of a control photon at very large optical depths, *i.e.* with more than 90% absorptive losses.

Here we show that large conditional cross-phase shifts *per* photon can be attained over lengths of a few Rydberg SAs with *weak* and *freely propagating* signal and control pulses. Conditional π phase modulations are found to occur over a wide parameter range and at relatively small optical depths. This hinges on polarization-selective nonlinearities occurring in cold Rydberg atoms under a specific

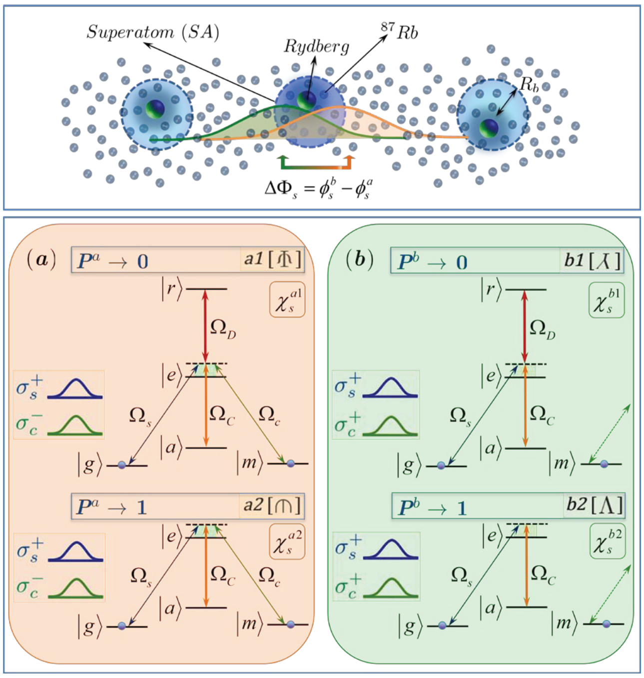

Fig. 1: (Color online) (***top***) *Conditional Cross-Phase Shift.* Different phase shifts ϕ_s^a and ϕ_s^b are imprinted upon a signal beam propagating across a *SA*, depending on the presence or absence of a control beam. The conditional cross-phase shift $\Delta\Phi_s$ may equal π for tens of SAs under a suitable *symmetric*-EIT configuration (*see text*). (***bottom***) *Cooperative Signal Susceptibilities.* Level configurations contributing to different cooperative signal susceptibilities, depending on the presence (*a1*-*a2*) or absence (*b1*-*b2*) of the control beam, being either choice conditional to its circular *polarization*. Each cooperative signal susceptibility is further determined by the SA *population* of the Rydberg state $|r\rangle$, whose two opposite limits $P^{a,b} \to 0$ and $P^{a,b} \to 1$ result in different level configurations and thus different individual signal susceptibilities $\chi_s^{a1,b1}$ and $\chi_s^{a2,b2}$. The levels $\{|g\rangle, |a\rangle, |m\rangle, |e\rangle$, and $|r\rangle\}$ represent the ^{87}Rb manifold $\{|5^2S_{1/2}, F=1, m=-1\rangle$, $|5^2S_{1/2}, F=2, m=0\rangle$, $|5^2S_{1/2}, F=1, m=+1\rangle$, $|5^2P_{1/2}, F=1, m=0\rangle$, and $|90s\rangle\}$ whose detunings from the dressing, coupling, signal, and control fields are $\delta_D = \omega_D - \omega_{re}$, $\delta_C = \omega_C - \omega_{ea}$, $\delta_s = \omega_s - \omega_{eg}$, and $\delta_c = \omega_c - \omega_{em}$ in order with $\Omega_{D,C,s,c}$ denoting the corresponding Rabi frequencies.

EIT-symmetric driving regime [26] and is at variance with cross-Kerr like [27], resonant absorbing [28], transversely separated [29], and site addressable [30] Rydberg nonlinearities. In the EIT-symmetric driving approach pursued here the pulsed regime is further shown to benefit from intrinsic group-velocity matching and high spatial-temporal coherence of signal and control beams. We finally discuss the feasibility of extending our scheme to work with small photon-numbers pulses subjecting to small losses and distortions, a critical step toward the implementation of a *deterministic* low intensity optical gate [31,32].

Phase-Shift. – We use cold Rydberg ^{87}Rb atoms driven by a pair of *strong* continuous-wave (CW) coupling and dressing fields into the level configurations shown in Fig. 1 to manage the phases of another pair of *weak* signal and control pulsed fields. Our scheme relies on three key features. *First*, the uppermost Rydberg level $|r\rangle$ coupled to the intermediate excited level $|e\rangle$ by the strong CW driving field Ω_D provides the large nonlinear mechanism. *Second*, the unpopulated ground state level $|a\rangle$ coupled to the intermediate excited level $|e\rangle$ by the strong CW coupling field Ω_C ensures that both the signal (Ω_s) and control (Ω_c) pulses always propagate in the EIT regime. *Third*, the equally populated ground state levels $|g\rangle$ and $|m\rangle$ allow for the *symmetric* response [33] experienced by the signal and control pulses (their role could actually be exchanged) and, in particular, it turns out to be crucial for their group-velocity matching.

Upon impinging on a sample of length L, a monochromatic signal beam of wavevector $k_s = \omega_s/c$ will acquire the nonlinear phase-shift $\phi_s = \phi_o Re[\chi_s]$, where $\phi_o = k_s L/2$ is half the vacuum phase-shift, and will experience absorption characterized by half the nonlinear optical depth $\kappa_s = \phi_0 Im[\chi_s]$ ($|\chi_s| \ll 1$). The signal susceptibility χ_s is found to depend critically on whether the Rydberg transition is *allowed* or *blocked*. The latter case occurs when one atom is excited to the Rydberg level and strong dipole-dipole interactions shift level $|r\rangle$ of other atoms within a SA far-off-resonance from field Ω_D (dipole blockade) [15]. When the control beam is present with the σ_c^- polarization [see Fig. 1(a)], atoms inside a *SA* are driven into a "Ѧ" or a "⋒" configuration respectively in the limit of small ($P^a \to 0$) or large ($P^a \to 1$) *SA* Rydberg excitations. Similarly, when the control beam is absent with the σ_c^+ polarization [see Fig. 1(b)], atoms inside a *SA* are driven into a "Λ" or a "Λ" configuration in the limit of small ($P^b \to 0$) or large ($P^b \to 1$) *SA* Rydberg excitations. The simpler "⋒" and "Λ" configurations occur because of dipole-blockade and most importantly, the *SA* Rydberg populations themselves strongly depend on whether the control beam is present (P^a) or absent (P^b), which triggers a very large cross-nonlinearity.

Such polarization-selective Rydberg nonlinearities can be exploited to bring about large conditional changes in the signal phase over a wide range of the coupling and dressing Rabi frequencies ($\Omega_{C,D}$) and detunings ($\delta_{C,D}$). In what follows, we choose to work with *equal* signal and control detunings $\delta_s = \delta_c \equiv \delta$, Rabi frequencies $\Omega_s = \Omega_c$, and ground levels $\{|g\rangle, |m\rangle\}$ populations, *i.e.* with a *symmetric*-EIT driving configuration [34]. We further adopt a universal relation for the dependence of the signal susceptibility χ_s on the *SA* Rydberg population $P^{a,b}$ akin to the one introduced in [17]. Then the signal phase-shift in the presence (ϕ_s^a) or absence (ϕ_s^b) of the control beam can be written as [38],

$$\phi_s^a = \phi_0\{\underbrace{P^a Re[\chi_s^{a2}] + (1-P^a) Re[\chi_s^{a1}]}_{Re[\chi_s^a]}\}, \ \{a1 \rightleftharpoons a2\} \quad (1)$$

$$\phi_s^b = \phi_0\{\underbrace{P^b Re[\chi_s^{b2}] + (1-P^b)Re[\chi_s^{b1}]}_{Re[\chi_s^b]}\}. \quad \{b1 \rightleftharpoons b2\} \quad (2)$$

Such relations are found to agree with rate equation models of multilevel Rydberg atoms exhibiting strong dipole-dipole interactions, based both on many-body simulations [17] and on semi-analytical one-body approaches [36]. In fact, they have been used to explain the observation of nonlinear dispersive effects in cold Rydberg atoms [7,37]. The phase shift ϕ_s^a depends on the susceptibility χ_s^a which we term here *cooperative* as it is determined by the interplay of the two *individual* susceptibilities χ_s^{a1} and χ_s^{a2} [34]. The susceptibility χ_s^a strongly depends on the SA Rydberg population P^a provided χ_s^{a1} is significantly different from χ_s^{a2}. The same holds for ϕ_s^b.

The population P^a specifically represents the averaged Rydberg excitation probability (sect. B of [34]), *i.e.* the Rydberg excited fraction for a single SA containing n_{SA} atoms [36]. In the presence of the control beam, for weak dressings the Rydberg population may decrease to $P^a \to 0$ so that the signal experiences the five-level ($\pitchfork$) dispersive shift $\phi_o Re[\chi_s^{a1}]$; conversely for intense dressings the Rydberg population may increase to $P^a \to 1$ so that the signal experiences the four-level ($\Cap$) dispersive shift $\phi_o Re[\chi_s^{a2}]$. The latter is based on the fact that an atom excited to the Rydberg level can detune from resonance all neighboring atoms inside a blockade sphere of radius R_b [36,39,40]. Analogous considerations hold for the population P^b and for the shift ϕ_s^b in Eq. (2) which will reduce in one case to $\phi_o Re[\chi_s^{b1}]$ ($\mathit{\Lambda}$) and in the other case to $\phi_o Re[\chi_s^{b2}]$ (Λ). It is further worth noting that for the specific *symmetric*-EIT driving configuration considered here, the signal exhibits almost identical responses for the Λ ($b2$) and the $\Cap$ ($a2$) configurations as well as for the Λ ($b1$) and the $\pitchfork$ ($a1$) configurations [35]. The conditional phase shift, *i.e.* the difference between the signal phase shift when the control is present ($a1 \rightleftharpoons a2$) and the signal phase shift when the control is absent ($b1 \rightleftharpoons b2$), then becomes,

$$\Delta\Phi_s = (\phi_s^b - \phi_s^a) \simeq \phi_0 \; Re[\chi_s^{b2} - \chi_s^{b1}] \times (P^b - P^a), \qquad (3)$$

where the challenge is to achieve $|\Delta\Phi_s| = \pi$. Individual susceptibilities χ_s^{b1} and χ_s^{b2} in Eq. (3) are defined in the absence of dipole-dipole interactions and can be computed by solving standard equations for atomic density matrix elements [41]. The Rydberg populations P^a and P^b, on the other hand, can be computed upon replacing $\Omega_{s,c} \to \Omega_{s,c}\sqrt{n_{sa}/2}$ with $n_{sa} = N_0(4\pi R_b^3/3)$ [39] in the corresponding equations for SA density matrix elements. Such a scaling takes into account the fact that the signal $\{|g\rangle \leftrightarrow |e\rangle\}$ and control ($\{|m\rangle \leftrightarrow |e\rangle\}$ transitions are enhanced by the atomic number $n_{sa}/2$ in relevant collective states of each SA, being the atoms equally distributed between ground levels $|g\rangle$ and $|m\rangle$.

These qualitative arguments are now quantified for a realistic sample of cold ^{87}Rb atoms. While details of the procedure used to compute both individual susceptibilities and Rydberg populations in Eq. (3) can be found in [34] for the case of monochromatic CW signal and control fields, we plot in Fig. 2 the resulting cross-phase shift as a function of the common detuning δ, the coupling Rabi frequency Ω_C [Fig. 2(a)] and the dressing Rabi frequency Ω_D [Fig. 2(b)], showing the characteristic parameter regions where $\Delta\Phi_s$ equals π. There we also plot the corresponding half-optical depth [38] showing maximal transmission $e^{-2\kappa_s} \simeq 87\%$ [Fig. 2(c)] for the driving configuration $\{\pitchfork - \Cap\}$ in Fig. 1(a) yet $e^{-2\kappa_s} \simeq 66\%$ [Fig. 2(d)] for the configuration $\{\mathit{\Lambda} - \Lambda\}$ in Fig. 1(b).

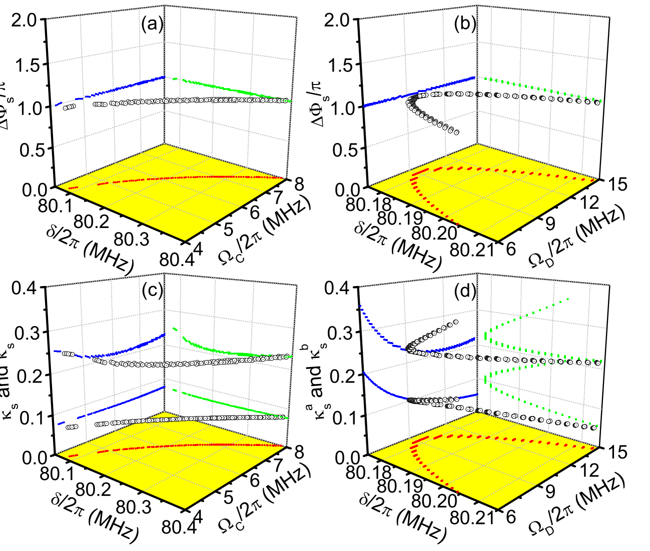

Fig. 2: (Color online) Cross-phase shifts ($\boldsymbol{a,b}$) and half-optical depths ($\boldsymbol{c,d}$) for CW signal and control fields vs. δ and Ω_C with $\Omega_D = 2\pi\times 12.0$ MHz ($\boldsymbol{a,c}$); δ and Ω_D with $\Omega_C = 2\pi\times 6.0$ MHz ($\boldsymbol{b,d}$). Black points in ($\boldsymbol{a,b}$) show the parameter regions where $\Delta\Phi_s = \pi$ along with the (*blue-red-green*) coordinate-planes projections. Black points in ($\boldsymbol{c,d}$) show the half-optical depths corresponding to $\Delta\Phi_s = \pi$ along with the (*blue-red-green*) coordinate-planes projections. The upper (lower) set of black points in ($\boldsymbol{c,d}$) are obtained in the absence (presence) of the control beam. The sample of cold ^{87}Rb atoms has a length $L = 1.0$ mm, a density $N_0 = 4.8\times 10^{12}$ cm^{-3}, dipole moments $d_{eg} = d_{em} = 1.5\times 10^{-29}$ Cm, and homogeneous dephasings: $\gamma_{ge,me,ae,re} = 2\pi\times 3.0$ MHz, $\gamma_{gr,mr,ar} = 2\pi\times 10$ kHz, and $\gamma_{ga,gm,ma} = 2\pi\times 2.0$ kHz. The CW coupling and dressing field have detunings $\delta_C = -\delta_D = 2\pi\times 80.0$ MHz.

The large shifts observed in Fig. 2 hinge on appreciable *differences* both in the (i) individual susceptibilities and in the (ii) Rydberg populations, as Eq. (3) suggests and also confirmed in ref. [34] through analytical and numerical computations. The former (i) arises from the fact that the signal experiences different dispersions in the Λ-type single-EIT regime ($b2$) and the $\mathit{\Lambda}$-type double-EIT regime ($b1$) [33], whereas the latter (ii) arises from the fact that Rydberg excitations, clearly occurring when the control is absent ($b1 \rightleftharpoons b2$), are instead largely suppressed when the control is present ($a1 \rightleftharpoons a2$). Such a quenching of the excitation probability P^a is due to the destructive interference between the competing excitation paths $\{|g\rangle \to |e\rangle \to |r\rangle\}$ and $\{|g\rangle \to |e\rangle \to |m\rangle \to |e\rangle \to |r\rangle\}$. This competing behavior is instead absent for P^b whereby the only excitation path is $\{|g\rangle \to |e\rangle \to |r\rangle\}$. It is to be noted that although the path $\{|g\rangle \to |e\rangle \to |m\rangle \to |e\rangle \to |r\rangle\}$ represents a high-order process, its contribution to the transition amplitude is nevertheless significant due to the enhanced SA Rabi frequencies ($\Omega_{s,c} \to \Omega_{s,c}\sqrt{n_{sa}/2}$) on the probe and control transitions shared by $n_{sa}/2$ atoms.

Reaching the π cross-phase shifts in Fig. 2 thus depends on the signal and control polarizations, through a careful selection of specific dispersive EIT regimes and specific Rydberg blockade effects. This polarization-sensitive blockade mechanism, in particular, is an important and novel feature that may be easily implemented to achieve large optical cross-nonlinearities in atomic media. Such a novelty could be especially appreciated through the comparison with familiar cross-nonlinear mechanisms without Rydberg blockade. This comparison is presented in [34], showing that the relevant $\Delta\Phi_s$ turns out to be orders of magnitudes smaller (as there is no appreciable differences on $\phi_s^{a,b}$ between the situations in which the control field is on or off) while $\kappa_s^{a,b}$ (indicating absorption) remain largely the same level. There we also discuss the influence of the Rydberg dephasings ($\gamma_{gr,mr,ar}$) on absorption.

Dynamics. – In a realistic signal and control fields setup one should consider *pulses* rather than monochromatic beams. The extension is not straightforward owing to typical pulse distortion effects [45] during the propagation in a dense dispersive sample of cold Rydberg atoms [7]. So we examine in the following the intrinsically time-dependent [11] cross-phase dynamics for narrow-band signal and control *pulses* under the same symmetric EIT driving conditions adopted before. The signal pulse slowly-varying envelope wave equation can be written as,

$$\frac{\partial\Omega_s^a}{\partial z}+\frac{1}{c}\frac{\partial\Omega_s^a}{\partial t} = \frac{i\pi N_0 d_{eg}^2}{2\epsilon_0\hbar\lambda_s}[P^a\sigma_{ge}^{a2}+(1-P^a)\sigma_{ge}^{a1}], \quad \{a1 \rightleftharpoons a2\} \tag{4}$$

$$\frac{\partial\Omega_s^b}{\partial z}+\frac{1}{c}\frac{\partial\Omega_s^b}{\partial t} = \frac{i\pi N_0 d_{eg}^2}{2\epsilon_0\hbar\lambda_s}[P^b\sigma_{ge}^{b2}+(1-P^b)\sigma_{ge}^{b1}]. \quad \{b1 \rightleftharpoons b2\} \tag{5}$$

The signal pulse evolution when the control pulse is on $\{a1 \rightleftharpoons a2\}$ or off $\{b1 \rightleftharpoons b2\}$ is determined by the coupled Maxwell-Liouville equations [46], including Eqs. (4-5) and relevant dynamic equations for the atomic coherences $\sigma_{ge}^{a1,a2,b1,b2}$ and for the *SA* Rydberg populations $P^{a,b}$, as discussed in detail in [34].

For a pair of identical signal and control *Gaussian* pulses, the signal amplitudes $|\Omega_s^{a,b}|$ are plotted in Fig. 3(a) $\{a1 \rightleftharpoons a2\}$ and in Fig. 3(b) $\{b1 \rightleftharpoons b2\}$. It is clear that the signal pulse experiences only slightly different losses, deformations, and time delays at the sample exit regardless of the control pulse. More interestingly, the signal phases $\phi_s^{a,b} = \arg(\Omega_s^{a,b})$ plotted in Fig. 3(c) $\{a1 \rightleftharpoons a2\}$ and in

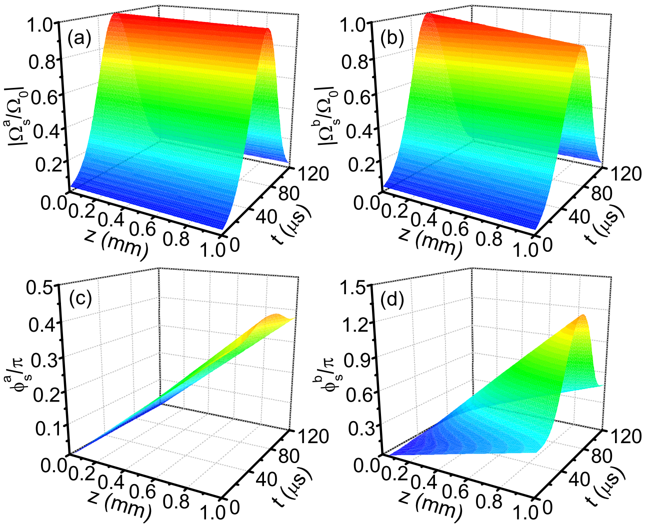

Fig. 3: (Color online) Spatial-temporal evolution of amplitudes (***a,b***) and phases (***c,d***) of a signal pulse in the presence (***a,c***) and absence (***b,d***) of another control pulse. Both incident pulses have the Gaussian profile $\Omega_{s,c}(t) = \Omega_0 e^{-(t-t_0)^2/\delta t^2}$ with $\Omega_0 = 2\pi \times 0.1$ MHz, $t_0 = 60$ μs, and $\delta t \simeq 32$ μs. Relevant parameters are the same as in Fig. 2 except $\Omega_C = 2\pi \times 6.0$ MHz, $\Omega_D = 2\pi \times 12.0$ MHz, and $\delta = 2\pi \times 80.19$ MHz.

Fig. 3(d) $\{b1 \rightleftharpoons b2\}$ turn out to be significantly inhomogeneous *or* roughly homogeneous depending on whether the control pulse is on *or* off. It should be stressed, in particular, that $\Delta\Phi_s$ as inferred from Fig. 3(c,d) cannot exceed $\sim 0.85\pi$, at variance with the value of π predicted by Fig. 2(a,b) in the steady-state case. One main reason is that absorptive loss is not negligible for the signal and control pulses during propagation.

Cross-phase shifts $\Delta\Phi_s$ close to π may still be reached, *e.g.*, through a slight change of the common detuning δ to enlarge its departure (190 kHz $\to$ 220 kHz) from the double EIT resonance. Fig. 4(a) shows the difference of individual signal phases (red-dashed), conditional to the Rydberg blockade occurrence, and the difference of SA Rydberg populations (blue-dotted), conditional to the control pulse polarization. They are so large that the corresponding cross-phase shift in Fig. 4(b) displays a maximum $\sim 0.96\pi$ (red-dashed). This maximum is nearly concomitant with the signal output peak and exhibits a 6% departure from the top for a 5% time variation around the center. It is worth stressing that the slow Rydberg decay affects further the evolution of Rydberg populations difference and thus cross-phase shift to result in a slow decay past the signal pulse. More homogeneous cross-phase shifts (blue-dotted) may be attained by using identical *flat-top* signal and control pulses [47]. Fig. 4(c) shows that signal amplitude losses are about 8% *or* 22% and signal time delays are about 1.8 μs *or* 5.8 μs, depending on whether the control pulse is on $\{a1 \rightleftharpoons a2\}$ *or* off $\{b1 \rightleftharpoons b2\}$. The SA populations in Fig. 4(d) for the $\{b1 \rightleftharpoons b2\}$ case follow nearly adiabatically the pulse excitation though this is less apparent at the trailing edge. One main reason is that the pulse excitation in a Λ configuration is faster than the Rydberg decay so that repopulating the ground levels becomes a slow process. This does not happen instead for the $\{a1\rightleftharpoons a2\}$ case (not shown) because the destructive quantum interference in a ⩚ configuration well prevents the Rydberg excitation.

It is worth noting that the results shown in Fig. 3-Fig. 4 correspond to pulses containing thousands of photons and to a cross-phase shift of about 1.0 mrad/photon for a beam waist of $w \simeq 12$ μm, which is an important figure of merit for tasks such as the realization of low-light-intensity cross-phase modulations. Thus, the results in Fig. 4(b) definitely represent a significant achievement [32] with the sample parameters suitable to state-of-the-art magneto-optical traps [48], while the prospect of obtaining sizable cross-phase shifts even with weaker signal and control pulses down to tens of photons hinges on the availability of denser Rydberg samples, yet with appropriate dephasing rates [34]. One main reason is that the variation of SA Rydberg populations P^a and P^b is determined by $n_{sa} \times \Omega_0^2/2$ so that a smaller Rabi frequency Ω_0 may be compensated through a larger atomic number n_{sa} per blockade sphere. Our scheme could also be adapted to the experimental setups based on cold atoms loaded into hollow-core optical fibers [49] and even solid-state setups such as Rydberg excitons in cuprous oxide [50, 51], thus promising practical applications. Phase noises, typically small if the incident pulses are prepared in the well stabilized coherent states, can be neglected when each contains tens to thousands of photons for the parameters used here. In fact, they just amount to additional dephasing rates (usually of the order of kHz) on relevant atomic transitions and thus have little effects on the present results.

Conclusions. – In summary, specific polarization-conditional cooperative nonlinearities that occur in far-off-resonance Rydberg-EIT media [26] can be harnessed to attain a π cross-phase shift ($\sim$0.001 rad per photon [52, 53]) between very weak signal and control light pulses that are intrinsically group-velocity matched. Such low-light-level large shifts are all-optically tunable, occur at small optical depths, and offer a possibility for future applications of deterministic optical gates with no need of optical cavities [7, 24, 25], storage and retrieval [23], or post-selection procedures [14, 23]. One main feature of our proposal is that the signal and control pulses always suffer small losses as they work either in the single-EIT regime or in the double-EIT regime, depending on whether the Rydberg excitation is allowed or blocked, which is further conditional to the polarization of the control pulse.

* * *

This work is supported by the National Natural Science Foundation (No.s 11534002, 11674049, and 61378094) and the 111 Project (No. B13013) of China. JHW, MA, and GLR would like to acknowledge the kind hospitality, respectively, in Pisa and in Changchun.

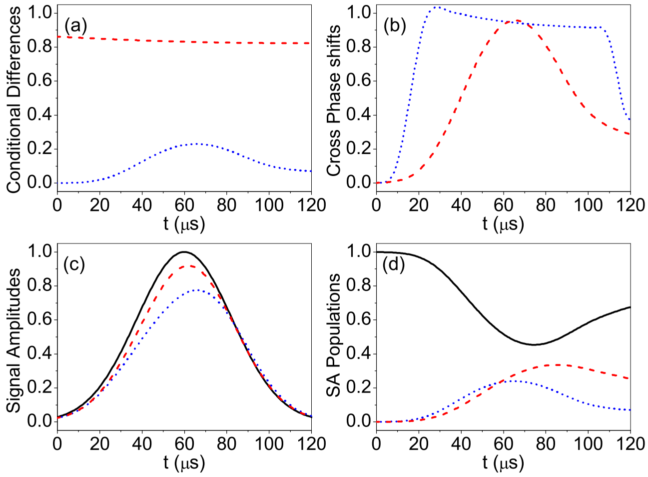

Fig. 4: (Color online) (***a***) Individual phases difference $0.2 \times \phi_0\, Re[\chi_s^{b2} - \chi_s^{b1}]/\pi$ (red-dashed) and SA populations difference $P^b - P^a$ (blue-dotted) at the sample exit for the Gaussian incident pulses as in Fig. 3. (***b***) Cross-phase shifts $\Delta\Phi_s/\pi$ at the sample exit for the Gaussian (red-dashed) incident pulses as in Fig. 3 and the flat-top (blue-dotted) incident pulses with a $\sim$ 90 μs duration. (***c***) Signal amplitudes at the sample exit in the presence (red-dashed) or absence (blue-dotted) of the control pulse, in reference to that at the sample entrance (black-solid). (***d***) SA populations of collective states $|g\rangle$ (black-solid), $|a\rangle$ (red-dashed), and $|r\rangle$ (blue-dotted) at the sample exit in the absence of the control pulse. Relevant parameters are the same as in Fig. 3 except $\delta = 2\pi \times 80.22$ MHz.

REFERENCES

[1] Agrawal G. P., *Nonlinear Fiber Optics* (Academic Press, New York) 2001.

[2] Matsuda N., Shimizu R., Mitsumori Y., Kosaka H. and Edamatsu K., *Nat. Photon.*, **3** (2009) 95-98.

[3] Nielsen M. A. and Chuang I. L., *Quantum Computation and Quantum Information* (Cambridge University Press, Cambridge) 2000.

[4] Milburn G. J., *Phys. Rev. Lett.*, **62** (1989) 2124-2127.

[5] Turchette Q. A., Hood C. J., Lange W., Mabuchi H., and Kimble H. J., *Phys. Rev. Lett.*, **75** (1995) 4710-4713.

[6] Reiserer A., Kalb N., Rempe G., and Ritter S., *Nature (London)*, **508** (2014) 237-241.

[7] Parigi V., Bimbard E., Stanojevic J., Hilliard A. J., Nogrette F., Tualle-Brouri R., Ourjoumtsev A., and Grangier P., *Phys. Rev. Lett.*, **109** (2012) 233602.

[8] Fushman I., Englund D., Faraon A., Stoltz N., Petroff P., and Vuckovic J., *Science*, **320** (2008) 769-772.

[9] Hammerer K., Sorensen A. S., and Polzik E. S., *Rev. Mod. Phys.*, **82** (2010) 1041-1093.

[10] Fleischhauer M., Imamoglu A., and Marangos J. P., *Rev. Mod. Phys.*, **77** (2005) 633-673.

[11] Shiau B.-W., Wu M.-C., Lin C.-C., and Chen Y.-C., *Phys. Rev. Lett.*, **106** (2011) 193006.

[12] Li S.-J., Yang X.-D., Cao X.-M., Zhang C.-H., Xie C.-D., and Wang H., *Phys. Rev. Lett.*, **101** (2008) 073602.

[13] Lo H.-Y., Chen Y.-C., Su P.-C., Chen H.-C., Chen J.-X., Chen Y.-C., Yu I. A., and Chen Y.-F., *Phys. Rev. A*, **83** (2011) 041804(R).

[14] Feizpour A., Hallaji M., Dmochowski G., and Steinberg A. M., *Nat. Phys.*, **11** (2015) 905-909.

[15] Lukin M. D., Fleischhauer M., Cote R., Duan L. M., Jaksch D., Cirac J. I., and Zoller P., *Phys. Rev. Lett.*, **87** (2001) 037901.

[16] Balewski J. B., Krupp A. T., Gaj A., Hofferberth S., Löw R., and Pfau T., *New J. Phys.*, **16** (2014) 063012.

[17] Ates C., Sevincli S., and Pohl T., *Phys. Rev. A*, **83** (2011) 041802(R).

[18] Petrosyan D., Otterbach J., and Fleischhauer M., *Phys. Rev. Lett.*, **107** (2011) 213601.

[19] Nielsen A. E. B. and Molmer K., *Phys. Rev. A*, **81** (2010) 043822.

[20] Petrosyan D. and Fleischhauer M., *Phys. Rev. Lett.*, **100** (2008) 170501.

[21] Firstenberg O., Peyronel T., Liang Q.-Y., Gorshkov A. V., Lukin M. D., and Vuletic V., *Nature(London)*, **502** (2013) 71-75.

[22] Pritchard J. D., Maxwell D., Gauguet A., Weatherill K. J., Jones M. P. A., and Adams C. S., *Phys. Rev. Lett.*, **105** (2010) 193603.

[23] Tiarks D., Schmidt S., Rempe G., and Durr S., *Sci. Adv.*, **2** (2016) e160036.

[24] Hacker B., Welte S., Rempe G., and Ritter S., *Nature(London)*, **536** (2016) 193-196.

[25] Beck K. M., Hosseini M., Duan Y. H., and Vuletic V., *PNAS*, **113** (2016) 9740-9744.

[26] Wu J.-H., Artoni M., and La Rocca G. C., *Phys. Rev. A*, **92** (2015) 063805.

[27] Friedler I., Petrosyan D., Fleischhauer M., and Kurizki G., *Phys. Rev. A*, **72** (2005) 043803.

[28] Gorshkov A. V., Otterbach J., Fleischhauer M., Pohl T., and Lukin M. D., *Phys. Rev. Lett.*, **107** (2011) 133602.

[29] He B., Sharypov A. V., Sheng J.-T., Simon C., and Xiao M., *Phys. Rev. Lett.*, **112** (2014) 133606.

[30] Paredes-Barato D. and Adams C. S., *Phys. Rev. Lett.*, **112** (2014) 040501.

[31] Ottaviani C., Vitali D., Artoni M., Cataliotti F., and Tombesi P., *Phys. Rev. Lett.*, **90** (2003) 197902.

[32] Li R.-B.,Zhu C.-J., Deng L., and Hagley E. W., *Appl. Phys. Lett.*, **105** (2014) 161103.

[33] Our symmetric driving may also be viewed as a symmetrically driven double-EIT configurations [see, *e.g.*, Joshi A. and Xiao M., *Phys. Rev. A*, **72** (2005) 062319].

[34] see the Supplemental Material for details.

[35] This has also been confirmed through numerical computations for the realistic Rydberg blockade sample we examine later [34].

[36] Garttner M., Whitlock S., Schonleber D. W., and Evers J., *Phys. Rev. A*, **89** (2014) 063407.

[37] Tanasittikosol M., Pritchard J. D., Maxwell D., Gauguet A., Weatherill K. J., Potvliege R.M., and Adams C. S., *J. Phys. B: At. Mol. Opt. Phys.*, **44** (2011) 184020.

[38] Similarly, replacing $Re[] \to Im[]$ in Eqs. (1-2) yields the absorption coefficients κ_s^b and κ_s^a.

[39] $R_b = \sqrt[6]{C_6 |\delta_D| / (|\Omega_C|^2 + |\Omega_D|^2)}$ is defined here by considering $V(R_b) = \hbar\gamma_{EIT}$ with $V(R) = \hbar C_6/R^6$ being the van der Waals potential at distance R and $\gamma_{EIT} = (|\Omega_C|^2 + |\Omega_D|^2)/|\delta_D|$ being the EIT linewidth associated with Rydberg excitation in the case of $|\delta_D| \gg \gamma_{ge}$ [21]. We have also considered in calculations that SA interactions will result in a reduction of the blockade radius [36], e.g., from $R_b \simeq 13.97$ μm ($n_{sa} = 27350$) to $R_b \simeq 13.27$ μm ($n_{sa} = 23250$) for the optimal parameters.

[40] The concept of an excitation blockade sphere [7,17], adopted here to get an intuitive picture of effects of the dipole-dipole interaction on the signal (control) quantum coherence, enables us to include Rydberg blockade effects in the cooperative susceptibilities $\chi_s^{a,b}$ in Eqs. (1-2).

[41] Scully M. O. and Zubairy M. S., *Quantum Optics* (Cambridge University Press, Cambridge) 1997.

[42] The control field propagates as in vacuum in the case of Fig. 1(b) while experiencing the same absorption as the signal ($\kappa_c^a = \kappa_s^a$) in the case of Fig. 1(a).

[43] Yan D., Liu Y.-M., Bao Q.-Q., Fu C.-B., and Wu J.-H., *Phys. Rev. A*, **86** (2012) 023828.

[44] Slowik K., Raczynski A., Zaremba J., Zielinska-Kaniasty S., Artoni M., and La Rocca G. C., *J. Mod. Opt.*, **58** (2011) 978-987.

[45] Artoni M. and Loudon R., *Phys. Rev. A*, **57** (1998) 622-628.

[46] Wu J.-H., Artoni M., and La Rocca G. C., *Phys. Rev. A*, **82** (2010) 013807.

[47] Venkataraman V., Saha K., and Gaeta L., *Nat. Photon.*, **7** (2013) 138-141.

[48] Sparkes B.M., Bernu J., Hosseini M., Geng J., Glorieux Q., Altin P.A., Lam P.K., Robins N.P. and Buchler B.C., *New J. Phys.*, **15** (2013) 085027.

[49] Langbecker M., Noaman M., Kjaergaard N., Benabid F., and Windpassinger P., *Phys. Rev. A*, **96** (2017) 041402.

[50] Kazimierczuk K., Frohlich D., Scheel S., Stolz H., and Bayer M., *Nature (London)*, **514** (2014) 343-347.

[51] Artoni M., La Rocca G. C., and Bassani F., *Europhys. Lett.*, **49** (2000) 445-451.

[52] At higher densities even steeper cross-phase shifts *per* photon can be achieved through a fewer-photons signal (control) pulse [34]. Dephasing effects, however, will start to become important with increasing densities [53].

[53] Gaj A., Krupp A. T., Balewski J. B., Low R., Hofferberth S., and Pfau T., *Nat. Commun.*, **5** (2014) 4546.